Supplementary Information

Proximity effects in Graphene and Ferromagnetic $CrBr_3$ van der Waals Heterostructure

Authors:

Sushant Kumar Behera[†], Mayuri Bora[†], Sapta Sindhu Paul Chowdhury, Pritam Deb[*]

Affiliations:

Department of Physics, Tezpur University (Central University), Tezpur-784028, India.

[*] Corresponding Author: pdeb@tezu.ernet.in(Pritam Deb).

[†] Authors have equal contribution.

1. Non-equilibrium Green function (NEGF) based formalism

The NEGF based formalism is selected in our case for precise and fast simulations in Gr-$CrBr_3$ based heterostructure system. The Poisson-Schrodinger equation has been solved self-consistently in case of NEGF formalism. The Green's function g is attributed by considering the energy matrices of left $\sum^{L}$ and right $\sum^{R}$ leads;

$$g(E) = \left[EI - H - \sum^{S} - \sum^{L} - \sum^{R}\right]^{-1} \tag{1}$$

where, I is attributed as identity matrix, $\sum^{S}$ is the scattering matrix, H is assigned as Hamiltonian of the system and E is ascribed as an energy eigen value. From equation (1), the broadening $(\wp L, \wp R)$ and spectral densities (D_L, D_R) can be evaluated as $\wp L, R = i[\sum L, R - \sum^{\dagger}_{L,R}]$ and $A_{L,R} = G(E)\wp L, RG^{\dagger}(E)$

For solving the Poisson equation the density matrix [Ɗ] is given by-

$$[Ɗ] = \int_{-\infty}^{\infty} \frac{dE}{2\pi}[A(E_{k,x})] f_0(E_{k,x} - \eta) \tag{2}$$

where, $A(E_{k,x})$ is defined as spectral density, $E_{k,x}$ is ascribed as the energy in the conduction region, η is attributed as chemical potential of the leads and $f_0(.)$ is the Fermi function. To implement NEGF formalism, Dirichlet and periodic boundary conditions must be employed in the leads and width of the heterostructure. The NEGF method can be evaluated using carrier density n_{tot} and substitute it into the Poisson equation to calculate self-consistently and iteratively calculate the potential U_{SCF}. To evaluate the transmission matrix the self-consistent converged values of the carrier density is used T (E, V)-

$$T(E,V) = Tr[A_{L\wp R}] = Tr[A_{R\wp L}] \tag{3}$$

The transmission channels are calculated by dividing coefficient into the bond contributions $T_{i,j}$. The channels are parted in such a way that the system is splitted in two parts a and b, then the channels across the periphery between a and b which sums to get the transmission coefficient as [ref]

$$T = \sum_{i \in a, i \in b} T_{i,j} \tag{4}$$

From equation (4), it signifies both positive and negative transmission contribution. A negative value interprets the backscattering of electron along the bond.

The transmission coefficient can be written as-

$$T_{nm} = \sum_{k} t_{nk} t^{t}_{km} \tag{5}$$

Therefore, in eq. (5), the transmission spectrum can be specified from the Bloch state Φ_n of the left lead to Bloch state Φ_k of the right lead is represented by transmission t_{nk}. The transmission coefficient is evaluated by taking the trace of transmission matrix

$$T = \sum_{n} T_{nn}$$

2. Scattering based approach

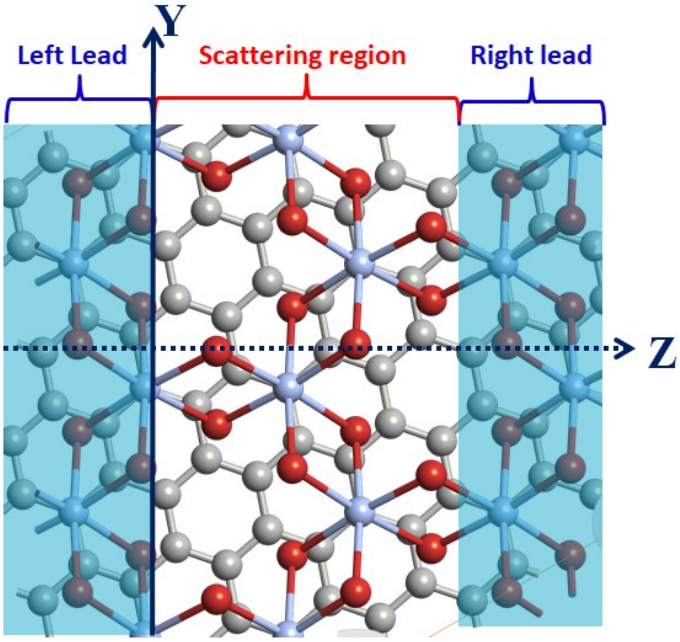

Scheme S1: Illustration of Gr-CrBr$_3$ heterolayer consisting three regions left lead, scattering region and right lead explained through Landauer-Buttiker scattering formalism

We investigated the ballistic transport in a quantum regime exhibiting the scattering region (0<z<L) along with the left (z<0) and right (z>L) leads. The electrons are supposed to move ballistically in the self-consistent potential consisting reflection as well as transmission which is controlled by the scattering region. In the *x-y* plane of the heterostructure system has a periodic repetition where the scattering region embodies propagating states with energy E having the same Bloch wave function which can be classified in k-index. Therefore, in considering large supercell in *x-y* plane limits the calculation in two-dimensional Γ point where k-index may be calculated separately. Moreover, the electrons considering spin-polarized state proceed independently in the self-consistent potential where the scattering formalism is solved independently for both the spin directions. However, our approach in Gr-$CrBr_3$ heterolayer system is to not consider any leads. But as shown in Scheme. S1 in the pristine bilayer system the extreme left and right unit cells are acted as corresponding left and right leads and the middle region corresponds to the scattering region, respectively. As the pristine bilayer system is magnetically active so the scattering based formalism for calculating the ballistic transmission spectrum is worthwhile.

In Scheme. S1, we consider a scattering state of Φ at energy E of a kohn-Sham equation [1]:

$$E\hat{S}|\Phi\rangle = \left[-\nabla^2 + V_{eff} + \hat{V}_{NL}\right]|\Phi\rangle, \qquad (1)$$

where, V_{eff} is refer to the effective local potential [2] and $\hat{V}_{NL}$is the non-local part

$$\hat{V}_{NL} = \sum_{\mathrm{Im}n} B^I_{mn}\left|\beta^I_m\right\rangle\left\langle\beta^I_n\right|, \qquad (2)$$

where β^I_m is associated with the set of projector functions for the Ith atom. The functions β^I_m are confined within the spheres of radius r_c for Ith atom. The B^I_{mn} coefficient depends on the used pseudopotential and local effective potential.

As energy E is kept fixed as an input parameter and can rewrite as follows:

$$E\Phi(r) = \left[-\nabla^2 + V_{eff}\right]\Phi(r) + \sum_{\mathrm{Im}n} \tilde{B}^I_{mn}\left\langle\beta^I_n\right|\Phi\rangle\beta^I_m(\vec{r} - \vec{R}_I), \qquad (3)$$

As mentioned, the translational symmetry of the scattering region is having typical Bloch wave function in *x-y* plane:

$$\Phi(\vec{r}_\perp + \vec{R}_\perp, z) = e^{ik_\perp \vec{R}_\perp}\Phi(r_\perp, z), \qquad (4)$$

A. Lead region

In the ballistic transmission model for Gr-$CrBr_3$ heterolayer is sandwiched between the left and the right leads (z<0, z>L), kept at a distance L. The leads and the scattering state Φ originates from Bloch wave function ϕ_b of the left lead can be written as:

$$\Phi = \begin{cases} \emptyset_b + \sum_{a \in L} r_{ab} \emptyset_{a}, z < 0 \\ \sum_{a \in R} t_{ab} \emptyset_{a}, z > L \end{cases} \qquad (5)$$

where, summation over a∈L (a∈R) incorporates the generalized propagating Bloch wave function in the left (right) lead with energy E which grow or decay towards the left (right) lead. Both propagating and evanescent Bloch states represents Complex band structure of a material which obeys the Bloch wave function in *x-y* plane. Therefore, beside the z-direction the translational symmetry does not exist which satisfies:

$$\phi_b(\overrightarrow{r_\perp}, z + l) = e^{ikl}\phi_b(\overrightarrow{r_\perp}, z),$$

(6) where, k is the complex number and l is length of the unit cell of the corresponding heterolayer. The corresponding wave functions ϕ_b for $Im\ k = 0$ and $Im\ k \neq 0$ illustrates the evanescent (decay or growth) and propagating states, respectively for evaluating complex band structure.

The general solution for the unit cell of the lead $z_0 < z < z_0 + l$ can be expressed as-

$$\phi_b(\vec{r}) = \sum_n c_{n,b} S_n(\vec{r}) + \sum_{\mathrm{Im}} c_{\mathrm{Im},b} S_{\mathrm{Im}}(\vec{r})$$

(7) where, S_n is independent of the homogenous equation-

$$ES_n(\vec{r}) = [-\nabla^2 + V_{eff}(\vec{r})]S_n(\vec{r}), \qquad (8)$$

where V_{eff} is the local effective potential and S_{Im} is the specific solution of the inhomogeneous equation:

$$ES_{\mathrm{Im}}(\overrightarrow{r}) = [-\nabla^2 + V_{eff}(\overrightarrow{r})]S_{\mathrm{Im}}(\overrightarrow{r}) + \sum_{\overrightarrow{R_\perp}} e^{i\overrightarrow{k_\perp}\overrightarrow{R_\perp}} \beta_m^I(\vec{r} - \overrightarrow{\tau^I} - \overrightarrow{R_\perp})$$

(9) Here, β_m^I is the set of projector function which is localized within the center of Ith atom, $\overrightarrow{\tau^I}$ is the position of the vector in the I^{th} atom of the unit cell. Both S_n and S_{Im} are periodic in *x-y* plane and sum over imaginary states necessitates all the projections in the unit cell.

The function of equation (7) can determine the coefficients of $c_{\mathrm{Im},b}$ which is given by-

$$c_{\mathrm{Im},b} = \sum_n \tilde{T}_{mn}^I \left\langle \beta_n^I \middle| \phi_b \right\rangle$$

(10) Therefore, k is the allowed values for a stated energy E which can be modify by equating eq. (2) along the *z*-direction of the function ϕ_b:

$$\phi_b(\overrightarrow{r_\perp}, z_0 + l) = e^{ikl}\phi_b(\overrightarrow{r_\perp}, z_0),$$

(11)

$$\phi'_b(\overrightarrow{r_\perp}, z_0 + l) = e^{ikl}\phi'_b(\overrightarrow{r_\perp}, z_0) \tag{12}$$

Thereafter, by equating eq. (3) in eqs. (10) - (12) it shows that the equations corresponds to the generalized eigen value can be expressed as-

CX=e^{ikl} DX,

(13) where, C and D are the matrices. To determine the generalized Bloch wave functions at energy E, the complex *k* components and coefficients of X needs to be solved.

B. Scattering region

The scattering state Φ lies in the region (0<*x*<L) which can be determined similar to that of the eq. (7):

$$\Phi(\vec{r}) = \sum_n c_n S_n(\vec{r}) + \sum_{\mathrm{Im}} c_{\mathrm{Im}} S_{\mathrm{Im}}(\vec{r}), \tag{14}$$

The scattering state Φ is fully illustrated by the coefficients $\{c_n, c_{Im}, r_{ab}, t_{ab}\}$. The coefficient c_{Im} can be illustrated by imposing the solutions of eqs. (8) and (9):

$$c_{\mathrm{Im}} = \sum_n \tilde{B}^I_{mn} \left\langle \beta^I_n \middle| \Phi \right\rangle$$

(15) Another set of equations on c_{Im} of the scattering region which intersects with the boundaries of the leads can be written as-

$$c_{\mathrm{Im}} = c_{\mathrm{Im},b} + \sum_a r_{ab} c_{\mathrm{Im},a} = \sum_n \tilde{B}^I_{mn} \left\langle \beta^I_n \middle| \Phi \right\rangle \tag{16}$$

and scattering region intersects in the plane *z*=0 can be written as-

$$c_{\mathrm{Im}} = \sum_n \tilde{B}^I_{mn} \left\langle \beta^I_n \middle| \Phi \right\rangle = \sum_a t_{ab} c_{\mathrm{Im},a} \tag{17}$$

Solving the eqs. (15)-(17) will give the unknown coefficients $\{c_n, c_{\mathrm{Im}}, r_{ab}, t_{ab}\}$.

C. Conductance Calculation

By considering the Landauer-Buttiker formalism, the conductance G in the ballistic regime is associated with the total transmission T near the Fermi energy is given by G=G$_0$T, where $G_0 = \frac{e^2}{h}$ is the conductance of quanta per spin. The total transmission is expressed as-

$$T = \sum_{ab} |T_{ab}|^2 = Tr[T^+T], \tag{18}$$

T is the normalized matrix for the transmission amplitudes $T_{ab} = \sqrt{I_a / I_b}\,.t_{ab}$, where I_b is the current probability of the Bloch wave function ϕ_b in the z-trajectory. The summation over a, b signifies the states of the polarized spin at the selected energy.

Therefore, to determine the unitary coefficients from the set of Bloch wave functions ϕ_b the eigen vectors of Hermitian matrix is considered in the conductance eigen channels. The Hermitian matrix is diagonal in the basis set of eigen values. So, the conductance can be expressed as-

$$G = G_0 \sum_a T_a$$

(19) where, T_a is the transmission probability for a^{th} eigen channel.

In this context, we need to calculate the total transmission T, the current I_b is propagated through the Bloch state ϕ_b in the z-trajectory. Therefore, in general the expression of current flowing can be written as-

$$I_b = I_b^0 - 2\,\mathrm{Im}\left[\sum_{\mathrm{Im}n} \widetilde{B}_{mn}^I \langle \beta_n^I | \phi_b \rangle \times \int_{-\infty}^{z_0} dz \oint \beta_m^I(\vec{r} - \vec{R}_I)\phi_b^*(\vec{r})\,d^2\vec{r}_\perp \right] \tag{20}$$

For every Bloch propagating state ϕ_b it should have $\sum_a T_{ab} + \sum_a R_{ab} = 1$, where T_{ab} and R_{ab} are the coefficients of transmission and reflection, respectively.

Further, the assumption from eq. (18) signifies that the current operator is diagonalized in the basis of Bloch wave function eventually which is not true. Merging of degenerate states may occur in same k in z-trajectory. Therefore, Bloch wave functions must be orthogonalized with respect to current operator before imposing in eq. (18) for obtaining the total transmission calculation. The current operator I_{bk} are given by-

$$I_{bk} = I_{bk}^0 + i\sum_{\mathrm{Im}n} \widetilde{B}_{mn}^I \left[\langle \beta_n^I | \phi_b \rangle \int_{-\infty}^{z_0} dz \oint \beta_m^I(\vec{r} - \vec{\tau}^I)\phi_b^*(\vec{r})\,d^2\vec{r}_\perp - \langle \beta_n^I | \phi_b \rangle * \int_{-\infty}^{z_0} dz \oint \left[\beta_m^I(\vec{r} - \vec{\tau}^I)\right] * \phi_b(\vec{r})\,d^2\vec{r}_\perp \right] \tag{21}$$

where,

$$I_{bk}^0 = -i\oint \left[\phi_b^*(\vec{r}_\perp, z_0) \frac{\partial \phi_b(\vec{r}_\perp, z)}{\partial z}\Big|_{z=z_0} - \frac{\partial \phi_b^*}{\partial z}\Big|_{z=z_0} \phi_b(\vec{r}_\perp, z_0) \right] d^2\vec{r}_\perp \tag{22}$$

Therefore, the conductance in ballistic regime is calculated in three different steps. In first, we perform the self-consistent calculation using plane-wave code to get the stable atomic configuration with screened potential V_{eff} and B_{mn}^I. Secondly, eq. (21) has been used to calculate the complex band structure of the propagating Bloch wave function with respect to the current operator. The unit cells of the lead are considered from the supercell of the pristine bilayer, which is not selected in the scattering region. Lastly, the transmission coefficients t_{ab} for rightward Bloch state ϕ_b of the left lead and obtain total transmission T in the eigen channel.

3. Interfacial Polarization

Van der Waals 2D heterostructure consists of heterogeneous mixtures of two or more constituents. In this structure, electric field polarization (known as the Maxwell-Wagner-

Sillars effect) [3] occurs in the interface of the heterostructure system. Thus, the externally applied electric field generates charge which is distributed over the interface of the heterostructure system and migrates at interface forming large dipoles. These induced dipoles exhibit enhanced inertia and require sufficient time (low field frequency) and thermal agitation to follow the alternation of the applied electric field.

The theoretical analysis of the phenomenon leads to a dipolar effect with an additional term regarding the possible contribution of the charges to the overall conductivity of the system. Interfacial polarization can be described by the equations [4]:

$$\varepsilon'(\omega) = \varepsilon_\infty + \frac{(\varepsilon_s - \varepsilon_\infty)\omega\tau}{1+\omega^2\tau^2} \tag{23}$$

$$\varepsilon''(\omega) = \frac{\sigma}{\varepsilon_0\omega} + \frac{(\varepsilon_s - \varepsilon_\infty)\omega\tau}{1+\omega^2\tau^2} \tag{24}$$

where ε_s, ε_∞ are the values of the real part of permittivity at low and high frequencies, σ the conductivity of the system, τ the relaxation time, ω the angular frequency of the applied electric field, and ε_0 the dielectric permittivity of free space (i.e. the interplanar spacing). Parameters ε_s, ε_∞, and σ are functions of the constituents' permittivity (ε_i), conductivity (σ_i), and volume fraction (v_i) and are given by the relations:

$$\varepsilon_s = \frac{\sum_i {}^{v_i\varepsilon_i'}\!\big/\!_{\sigma_i^2}}{(\sum_i {}^{v_i}\!\big/\!_{\sigma_i})^2} \tag{25}$$

$$\varepsilon_\infty = \frac{1}{(\sum_i {}^{v_i}\!\big/\!_{\varepsilon_i'})} \tag{26}$$

$$\sigma = \frac{1}{(\sum_i {}^{v_i}\!\big/\!_{\sigma_i})} \tag{27}$$

Interfacial polarization is present in 2D heterostructure, especially in the case of a conductive reinforcing phase because of the coexistence of heterogeneous interfaces and stable crystalline phases [5]. The dramatic increase in interfacial area in heterostructures sets interfacial polarization as a predominant physical effect for their electrical performance.

Relaxed Supercell used in calculations:

Table S1:

Bravais Lattice: Hexagonal

Lattice parameters:

a = 6.34 Å, c = 45.11 Å

Coordinates of atoms in supercell (fractional coordinates)

C	0.238096	0.047619	0.557630
C	0.476191	0.095238	0.557630
C	0.952381	0.190476	0.557630
C	0.190476	0.238095	0.557630
C	0.666667	0.333333	0.557630
C	0.904762	0.380953	0.557630
C	0.380953	0.476190	0.557630
C	0.619048	0.523810	0.557630
C	0.095238	0.619047	0.557630
C	0.333334	0.666667	0.557630
C	0.809524	0.761905	0.557630
C	0.047619	0.809524	0.557630
C	0.523810	0.904762	0.557630
C	0.761905	0.952381	0.557630
Br	0.523866	0.166667	0.505976
Br	0.171406	0.519127	0.505976
Br	0.818946	0.814207	0.505976
Cr	0.838073	0.500000	0.474163
Cr	0.504739	0.833334	0.474163
Br	0.819116	0.166667	0.442369
Br	0.523696	0.518957	0.442369
Br	0.171406	0.814377	0.442369

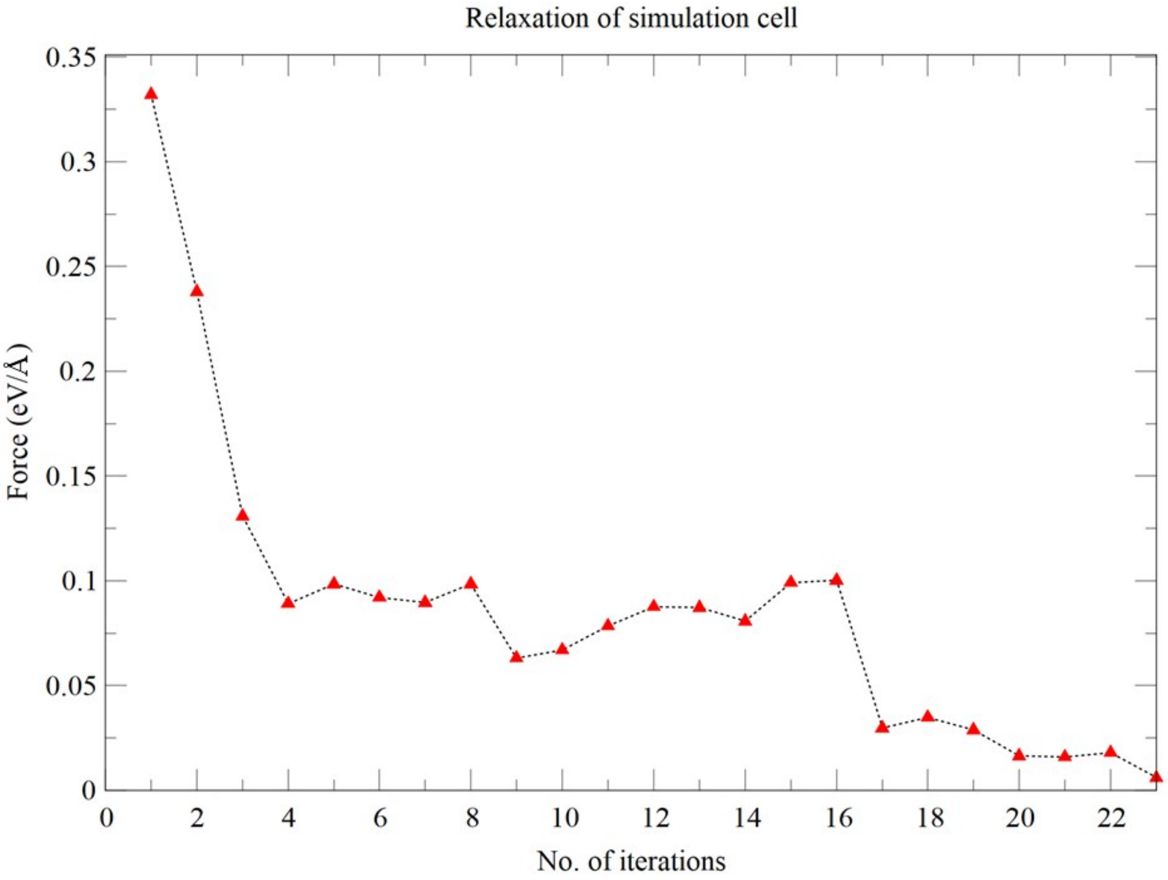

Figure S1: Relaxation of simulation cell by BFGS method upto an interatomic force of 0.01 eV/Å.

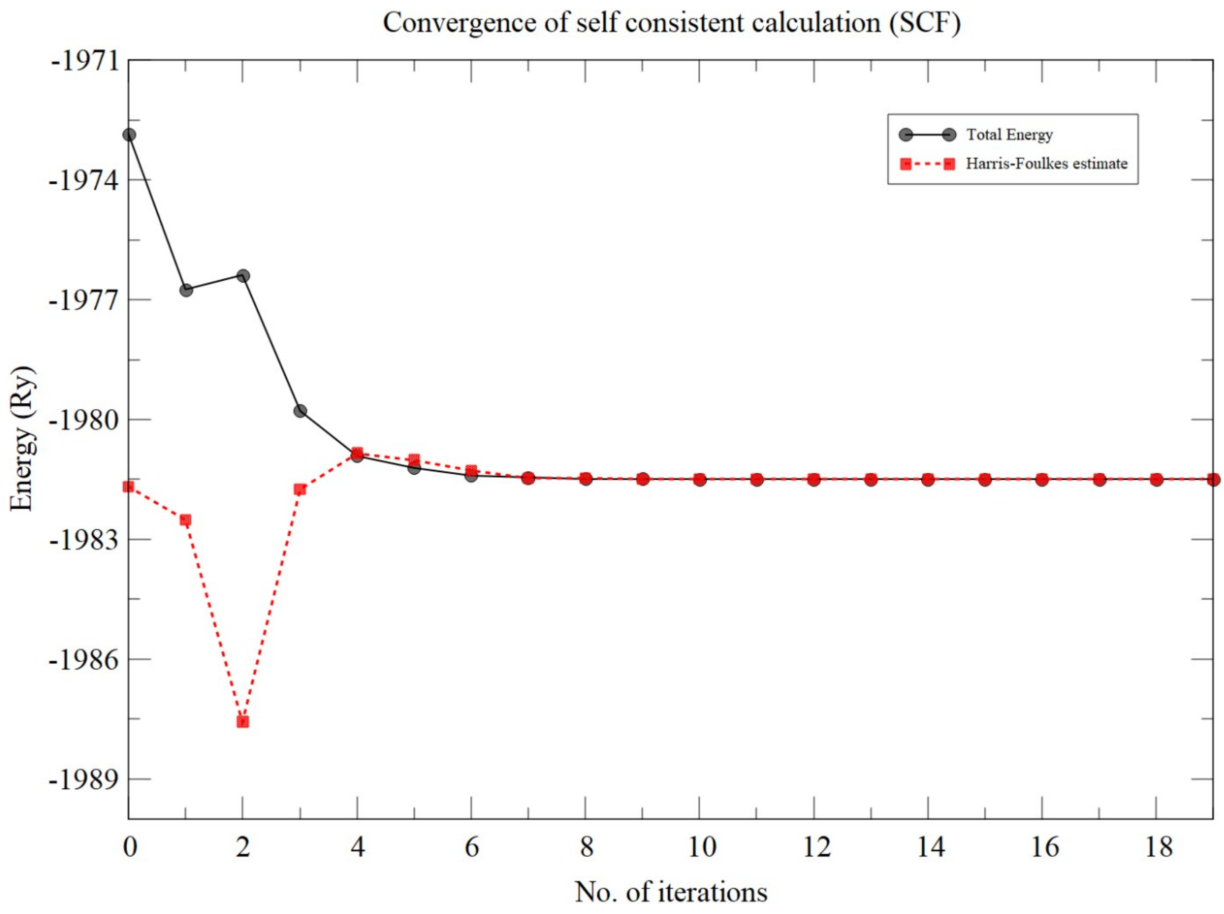

Figure S2: Convergence of SCF for further density of states and band structure calculations.

Charge density contour profile for Gr-CrBr$_3$ heterostructure system

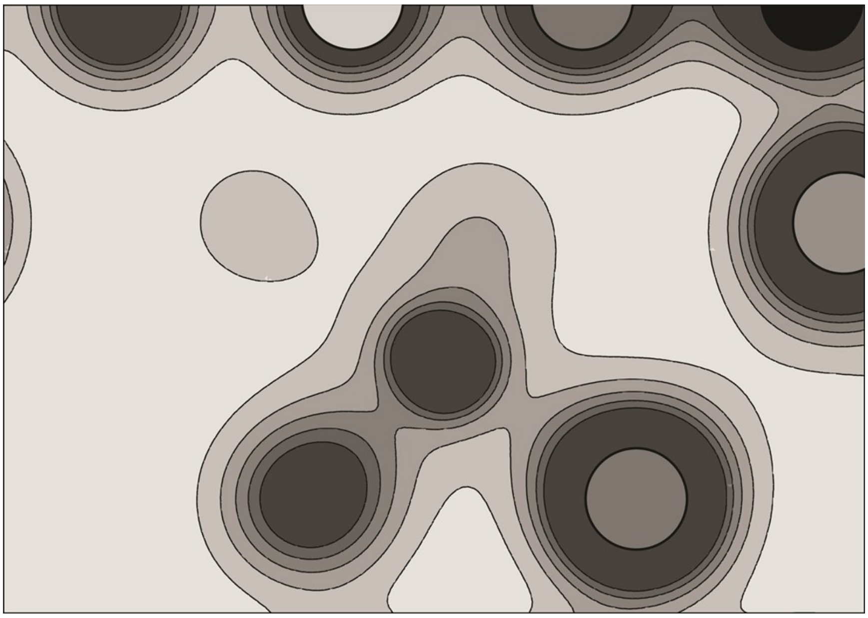

Figure S3: Charge density contour plot of Gr-CrBr$_3$ heterostructure.

Modulation of split-off energy gap with the variation of external electric field in reverse and forward bias in Gr-$CrBr_3$ heterostructure

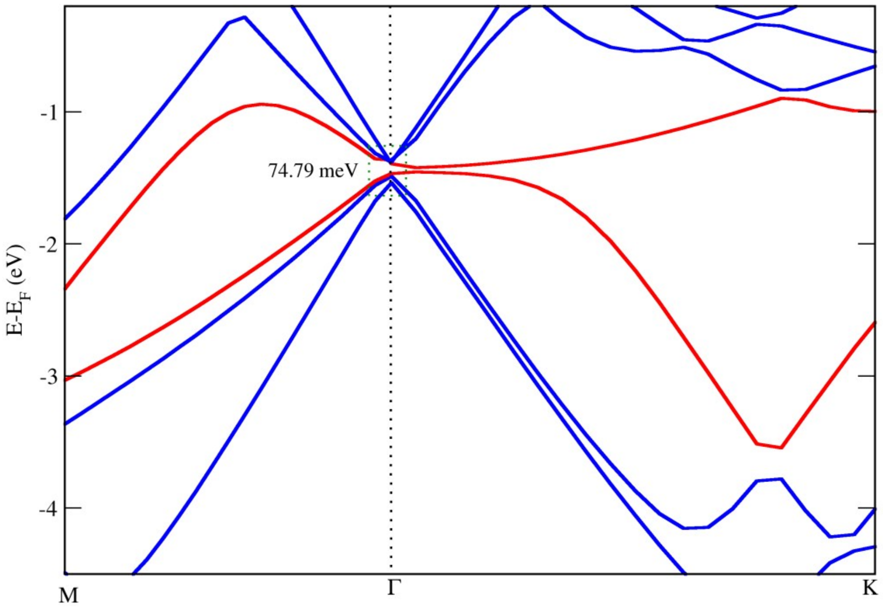

Figure S4: The Band diagram Gr-$CrBr_3$ heterolayer at 0.1 V/Å.

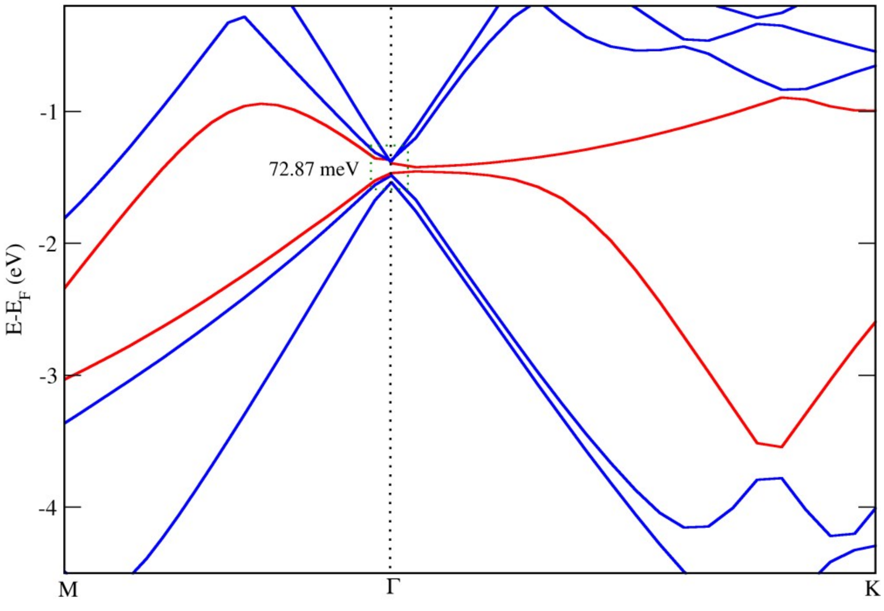

Figure S5: The Band diagram Gr-$CrBr_3$ heterolayer at -0.1 V/Å.

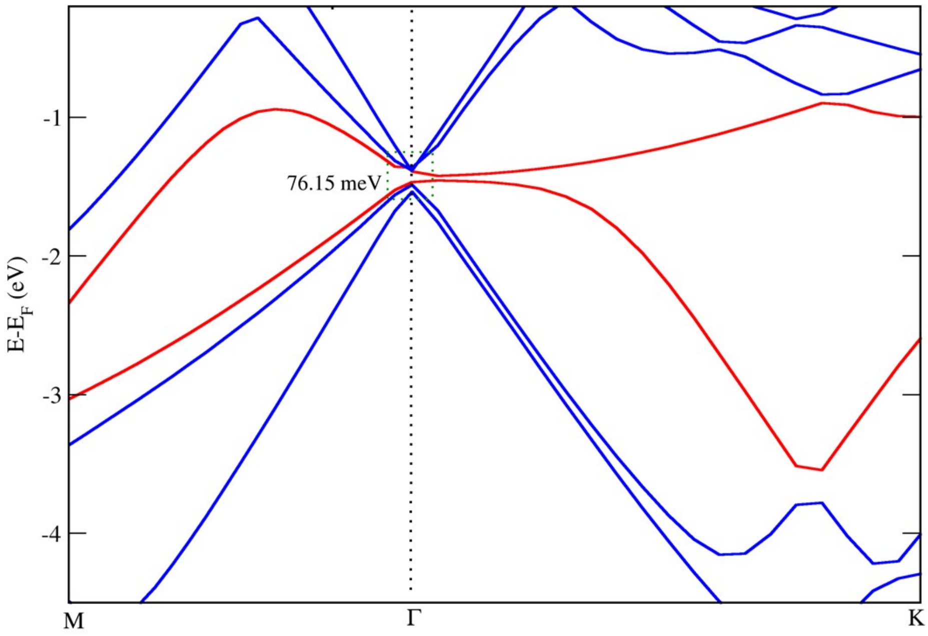

Figure S6: The Band diagram Gr-CrBr$_3$ heterolayer at 0.2 V/Å.

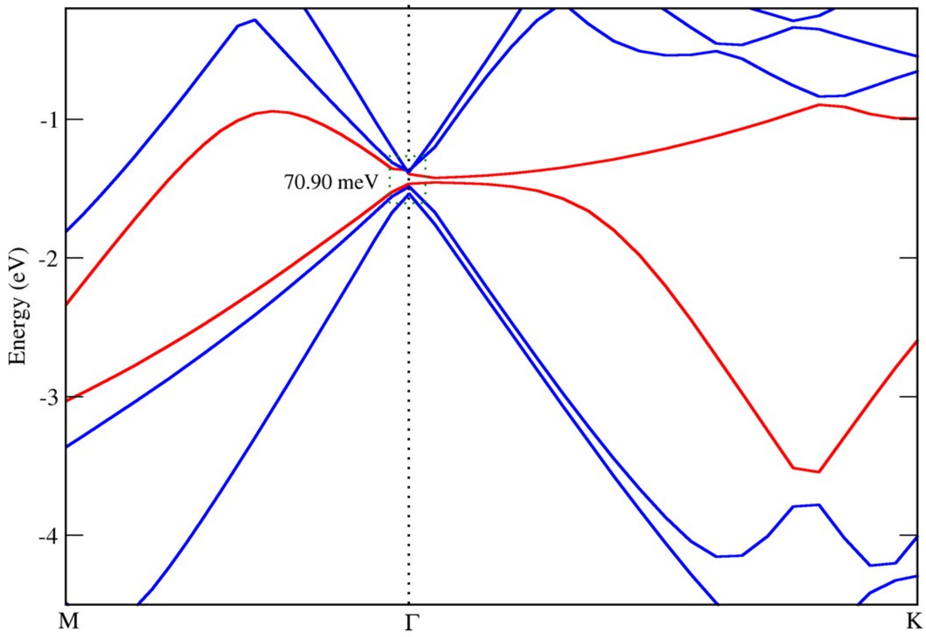

Figure S7: The Band diagram Gr-CrBr$_3$ heterolayer at -0.2 V/Å

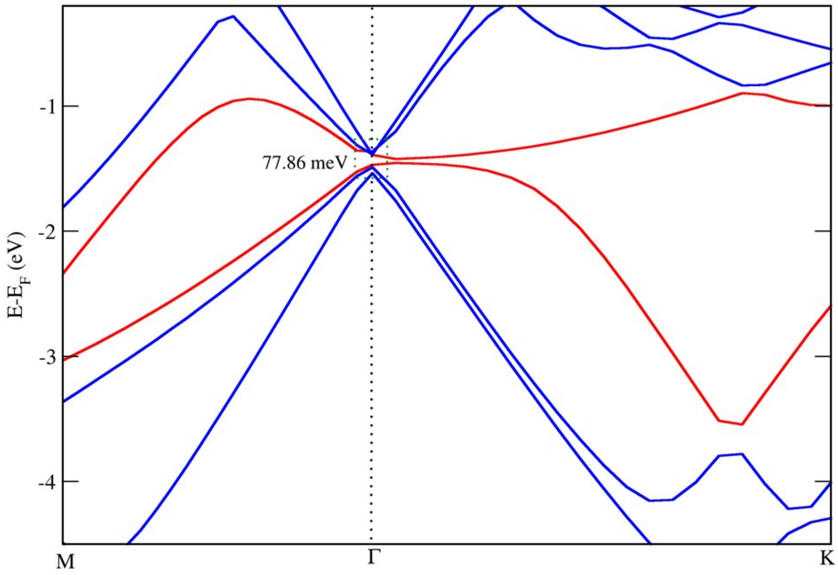

Figure S8: The Band diagram Gr-CrBr$_3$ heterolayer at 0.3 V/Å

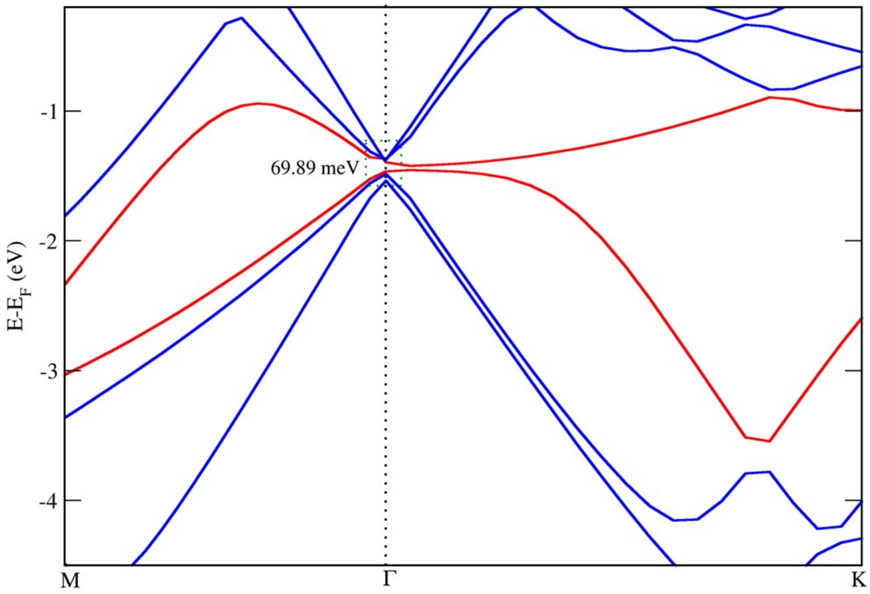

Figure S9: The Band diagram Gr-CrBr$_3$ heterolayer at -0.3 V/Å

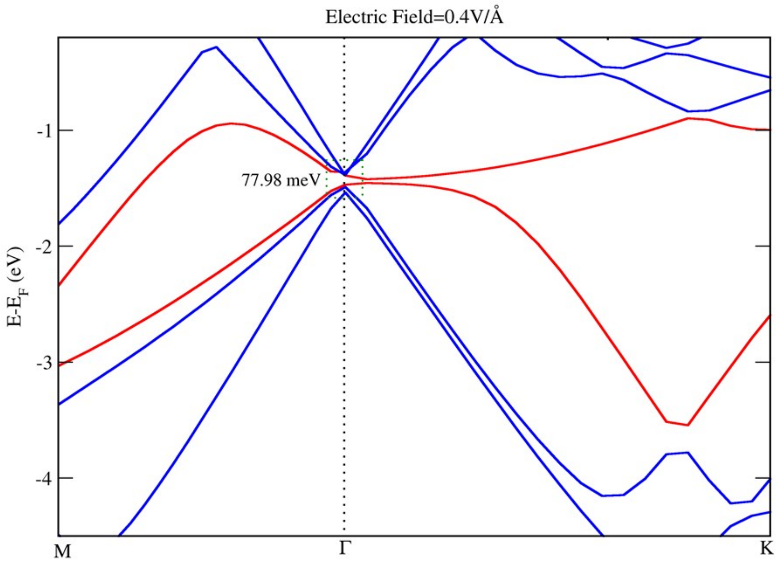

Figure S10: The Band diagram Gr-CrBr$_3$ heterolayer at 0.4 V/Å

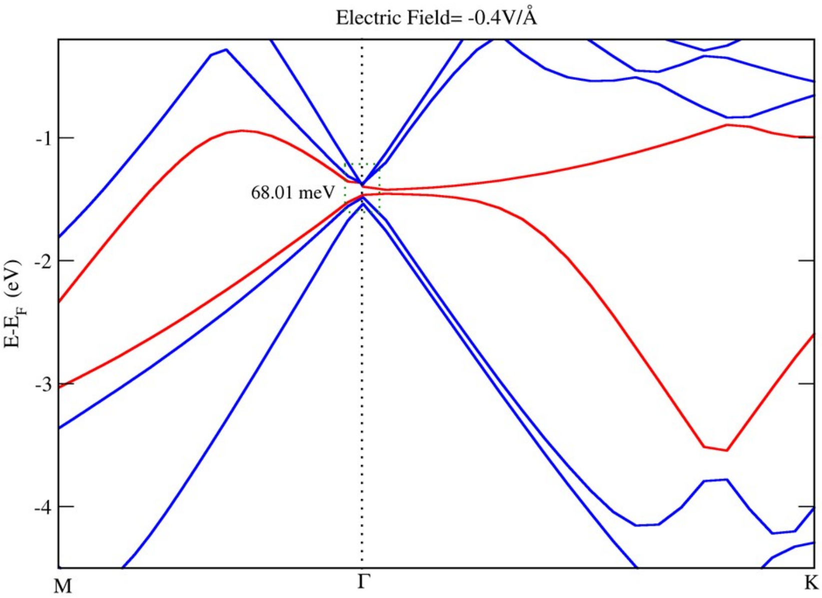

Figure S11: The Band diagram Gr-CrBr$_3$ heterolayer at -0.4 V/Å

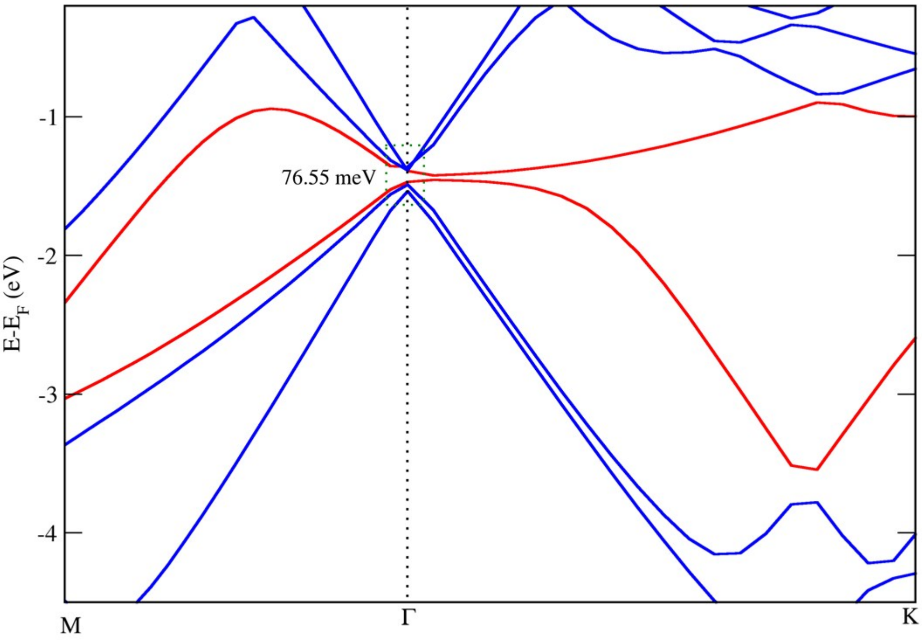

Figure S12: The Band diagram Gr-CrBr$_3$ heterolayer at 0.5 V/Å

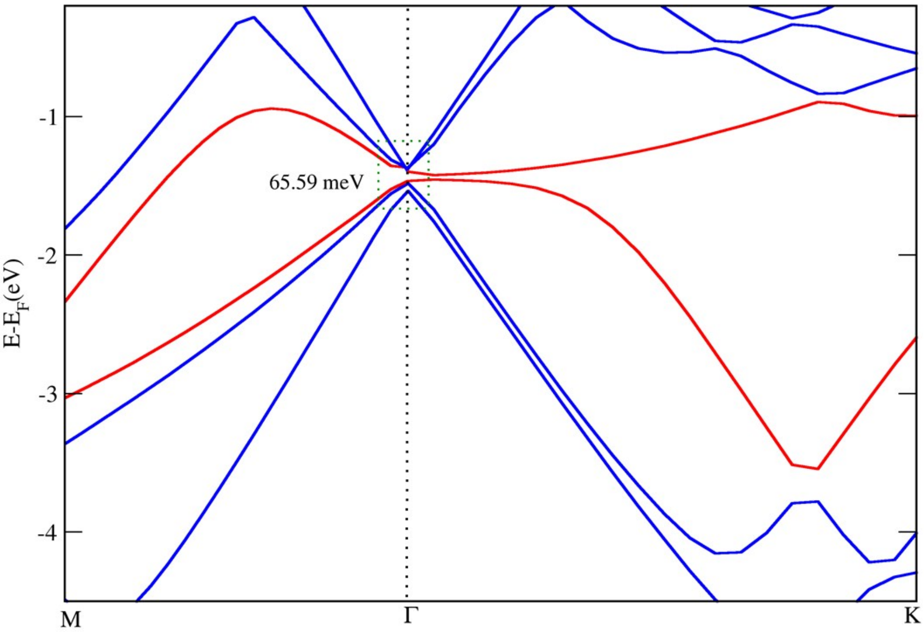

Figure S13: The Band diagram Gr-CrBr$_3$ heterolayer at -0.5 V/Å

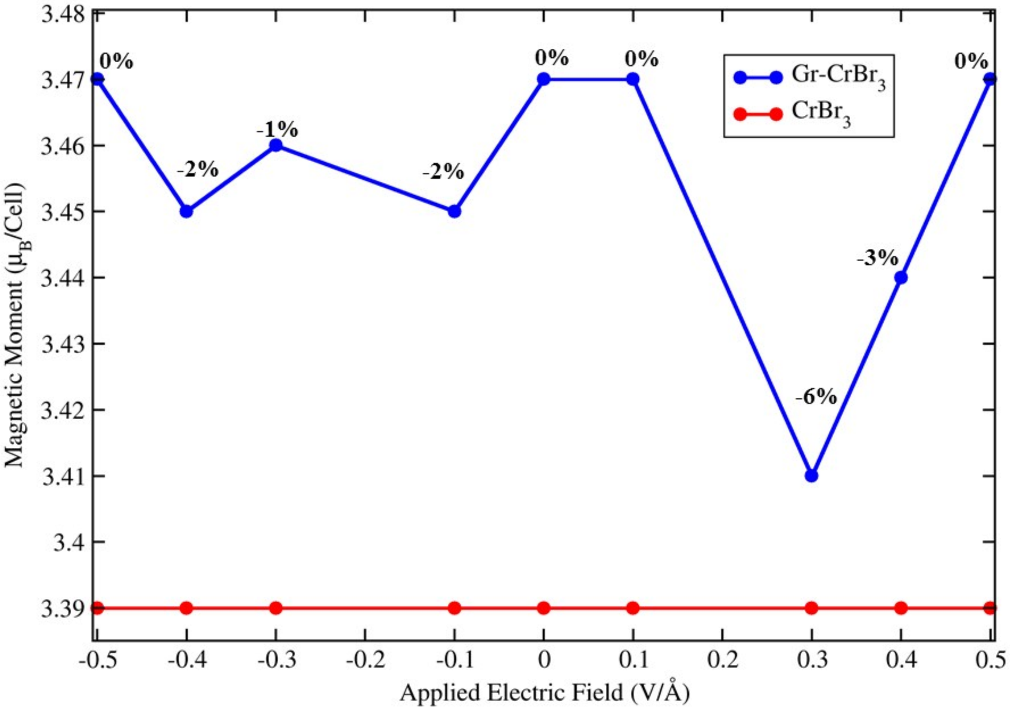

Figure S14: The modulation in magnetic moment value of the heterostructure in presence of external electric field (Z direction). The applied field is varied between 0 to 0.5V/Å in forward biasing direction and varied between 0 to -0.5V/Å in reverse biasing direction. The same results for $CrBr_3$ monolayer sheet is shown for comparison purpose.

References

1 K. Laasonen, A. Pasquarello, R. Car, Ch. Lee, and D. Vanderbilt, *Phys. Rev. B*, 1993, **47**, 10142.

2 D. Vanderbilt, *Phys. Rev. B*, 1990, **41**, 7892.

3 D. J. Mickish, *J. Appl. Phys*., 1979, **50**, 5923.

4 A. R. von Hippel, Dielectrics and Waves, Artech, Boston, MA, 1995.

5 P. A. M. Steeman, J. van Turnhout, Dielectric properties of inhomogeneous media, in: F. Kremer, A. Schonhals (Eds.), Broadband Dielectric Spectroscopy, Springer, Berlin, 2003, pp. 495-522.